Energy-Efficient Translucent Optical Transport Networks With Mixed Regenerator Placement

Zuqing Zhu, *Senior Member, IEEE*, Xiaoliang Chen, Fan Ji, Liang Zhang, Farid Farahmand, *Member, IEEE*, and Jason P. Jue, *Senior Member, IEEE*

***Abstract*—Translucent networks utilize sparse placements of optical–electronic–optical (O/E/O) 3R (reamplification, reshaping, and retiming) regenerators to improve the cost effectiveness and energy efficiency of wavelength-routed optical transport networks. In this paper, we show that the energy cost of a translucent network can be further reduced by leveraging the energy efficiency of all-optical 2R (reamplification and reshaping) regenerators. We propose a translucent network infrastructure that uses all-optical 2R regenerators to partially replace O/E/O 3R regenerators and implements mixed regenerator placements (MRP).**

We first consider the problem of MRP along a single given path, and propose three path-based impairment-aware MRP algorithms, based on periodic placement, genetic algorithm (GA), and ant colony optimization (ACO). We then address the offline network planning problem and develop a heuristic algorithm. By incorporating with one of the proposed MRP algorithms, the heuristic can achieve joint optimization of MRP and routing and wavelength assignment for high energy efficiency. We design simulations to compare the performance of different offline network planning scenarios and to see which one can provide the best balance between quality of transmission and energy cost. Simulation results show that the algorithm achieves 58.91–73.62% saving on regeneration energy, compared to the traditional scheme without all-optical 2R regenerators. The results also indicate that the joint optimization using the MRP-GA obtains the best network planning in terms of energy efficiency. Finally, we address the problem of online provisioning, and propose several algorithms to serve dynamic lightpath requests in translucent networks with MRP, and implement them in simulations to compare their performance in terms of blocking probability. Simulation results indicate that the online provisioning algorithm that utilizes the combination of the MRP-GA and a multiple MRP scheme achieves the lowest blocking probability.

***Index Terms*—Ant colony optimization (ACO), energy-efficient optical networks, genetic algorithm (GA), mixed regenerator placement (MRP), network planning and provisioning, translucent optical networks.**

I. Introduction

OVER the past decade, the overwhelming growth of Internet traffic has stimulated intensive research and development on high-speed optical transport networks. To combat with transmission impairments, network operators originally relied on optical–electronic–optical (O/E/O)-based 3R (reamplification, reshaping, and retiming) regenerators at every switching node to improve the signal quality of each wavelength channel. This type of opaque network infrastructure was expensive and power-hungry due to the frequent involvement of O/E/O 3R regenerators. With wavelength division multiplexing (WDM) technology and advances in erbium-doped fiber amplifiers (EDFA), huge bandwidth transmission at low cost was achieved over a single fiber by introducing optical transparency in the physical layer. To this end, operators started to migrate their networks from opaque to translucent, in order to reduce capital expenditures (CAPEX) and operational expenditures (OPEX) [1]. The objective of translucent network design is to utilize sparse placement of O/E/O 3R regenerators for achieving improved cost effectiveness and energy efficiency [1], [2]. However, as O/E/O 3R regenerators are removed from the intermediate nodes of a lightpath, transmission impairments may accumulate and eventually limit the transmission reach when the received signal quality [e.g., bit error rate (BER)] is unacceptable. Therefore, translucent network design has to balance the tradeoff between performance and cost [2], [3].

The concept of translucent optical network was first proposed in [1], where Ramamurthy *et al.* proved that translucency could help to reduce blocking probability for medium-scale WDM networks. The work was extended in [2], where an architecture of the translucent regeneration site was discussed. Shen *et al.* investigated the placement of electronic switches in translucent networks and proposed a heuristic for routing and wavelength assignment (RWA) based on a 2-D Dijkstra algorithm to reduce blocking probability. To operate translucent networks, a dynamic resource allocation and routing scheme was proposed in [4]. The scheme was realized through dynamically sharing regeneration resources between regeneration and access functions under a hierarchical translucent network model. Dimensioning of translucent networks was investigated in [5], and the authors proposed a hybrid link/path-based network design approach to reduce the number of O/E/O 3R regenerators in the network. In [6], Pachnicke *et al.* proposed an online impairment-aware routing algorithm that considered both linear and nonlinear fiber transmission impairments in translucent networks. Several integer linear programming (ILP) models were formulated in [7] to solve the offline regenerator placement and impairment-aware RWA problem in translucent networks. This work was extended in [8] by the same authors, and several joint online RWA and regenerator allocation algorithms were developed to provision translucent networks with the consideration of quality of transmission (QoT). Sparse traffic grooming in translucent networks was investigated in [9], where Shen *et al.* formulated several mixed-integer linear programming (MILP) models

Manuscript received May 29, 2012; revised July 31, 2012; accepted August 03, 2012. Date of publication August 15, 2012; date of current version September 26, 2012. This work was supported in part by the Program for New Century Excellent Talents in University under Project NCET-11-0884 and in part by the Natural Science Foundation of Anhui Province under Project 1208085MF88.

Z. Zhu, X. Chen, F. Ji, and L. Zhang are with the School of Information Science and Technology, University of University of Science and Technology of China, Hefei, Anhui 230027, China (e-mail: zqzhu@ieee.org; arabus@mail.ustc.edu.cn; angelajf@mail.ustc.edu.cn; mnizh@mail.ustc.edu.cn).

F. Farahmand is with the Department of Engineering Science, Sonoma State University, CA 94928 USA (e-mail: farid.farahmand@sonoma.edu).

J. P. Jue is with the Department of Computer Science, University of Texas at Dallas, TX 75080 USA (e-mail: jjue@utdallas.edu).

Digital Object Identifier 10.1109/JLT.2012.2213296

to optimize subwavelength traffic grooming and developed a heuristic for regenerator placement. The translucent network design with mixed line rates of 10/40/100 Gb/s was discussed in [10], and an ILP model was formulated to optimize regenerator placement. In [11], experimental demonstration of dynamic provisioning of lightpaths was achieved in a GPMLS-enabled translucent network with sparse O/E/O 3R regenerators placement. Azodolmolky *et al.* developed an impairment-aware RWA algorithm that considered QoT estimation inaccuracy in translucent networks [12], and they also experimentally demonstrated an impairment-aware network planning and operation tool for transparent/translucent networks [13]. An auxiliary graph-based regenerator placement and RWA approach was proposed in [14], and reduction of wavelength changes was demonstrated. Zhu *et al.* investigated multicast in translucent networks and developed an impairment-aware regenerator placement algorithm for light trees [15]. On top of these works that investigated various aspects of the design and provisioning of translucent networks, Saradhi *et al.* summarized practical and deployment issues of regenerator placement [3], and Sambo *et al.* reviewed reconfigurable optical add/drop multiplexer (ROADM) architectures and related constraints [16].

Most of the aforementioned works relied solely on O/E/O 3R regenerators to solve the QoT and wavelength contention issues in translucent networks. It has already been experimentally demonstrated that all-optical 2R regenerators can improve QoT in a more cost-effective and energy-efficient manner [17]–[19]. Moreover, the majority of these devices perform signal regeneration through all-optical wavelength conversion [17], and therefore can resolve wavelength contention simultaneously. These types of optical devices, such as semiconductor optical amplifier-based Mach–Zehnder interferometers (SOA-MZI), have been experimentally demonstrated for operation speeds at 40 Gb/s and beyond [17], and have become commercially available [19]. Therefore, we expect that all-optical 2R regenerators based on them will emerge for optical transport networks in the near future. To take advantage of these benefits, we recently proposed an energy-efficient translucent network infrastructure that used all-optical 2R regenerators to partially replace O/E/O 3R regenerators and implemented mixed placements of EDFAs (1R), all-optical 2R regenerators, and O/E/O 3R regenerators [20]–[23]. Simulation results indicated that the proposed mixed regenerator placement (MRP) approach could effectively reduce the number of O/E/O 3R regenerators in networks, and therefore achieve green translucent network designs. In this paper, we extend our previous work by proposing several path-based impairment-aware MRP algorithms that can further improve networks' energy efficiency and can provide a better balance between QoT and energy cost. Based on the algorithms, we investigate offline planning and online provisioning of translucent networks with MRP, and incorporate joint optimization of regenerator placement/allocation and RWA to obtain network performance improvements.

The rest of this paper is organized as follows. Section II introduces the principle of mixed placement of 1R/2R/3R regenerators in translucent networks and discusses the path-based impairment-aware MRP algorithm. Section III investigates the offline network planning with joint optimization of MRP and RWA. The online provisioning of the energy-efficient translucent networks with MRP is addressed in Section IV. Finally, Section V summarizes this paper.

II. Mixed Placement of Optical 1R/2R/3R Regenerators

In this paper, we consider two types of nodes in translucent networks: the regeneration sites and the switching nodes. Fig. 1 illustrates the node architectures for supporting MRP. Located on the fiber links between switching nodes, the regeneration sites do not have switching capability and are for by-pass traffic only. The switching nodes are the places where lightpaths can start and end and the routing of traffic is performed. We reserve four ports in each switching node and configure them with loop-back fibers to incorporate MRP. Since each 2R or 3R regenerator can only handle a single-wavelength channel, we insert wavelength-division multiplexers and demultiplexers in the system architectures to facilitate wavelength selection and wavelength switching. Within both types of nodes, when the signal does not experience any regenerative device (i.e., all-optical 2R or O/E/O 3R regenerator), it is reamplified (1R) only with EDFAs.

A. Operation Principle of MRP

We assume that the optical signal is in an ON–OFF keying (OOK) format, and we use BER as the QoT indicator. Consider a WDM topology $G(V, E)$, where V is the node set and E is the fiber link set. For a lightpath from node s to d that goes across a few nodes in G, the signal can be assigned to an all-optical 2R regenerator, or an O/E/O 3R regenerator, or nothing (1R) at each intermediate node $u \in V$. Therefore, in the path domain, the regenerator placement of the lth lightpath from s to d can be modeled with a flag $f_{s,d,l}^{i,u}$, where $i = 1, 2, 3$ for 1R, 2R, and 3R regenerators, respectively. $f_{s,d,l}^{i,u} = 1$ if the signal is regenerated by the corresponding type of regenerator at node u; otherwise, it equals 0.

With $\{f_{s,d,l}^{i,u}\}$ of intermediate nodes along the routing path and the characteristics of fiber links that are in use, we can estimate the BER evolution of the signal in a hop-by-hop manner using the BER model formulated in [21] and [24]. Note that most of the previous works on BER estimation in translucent networks assumed that a signal's BER is restored after an O/E/O 3R regenerators. However, both theoretical [24], [25] and experimental results [17], [26] have suggested that signal regeneration cannot restore BER without the forward-error-correction (FEC) functionality. For those 3R regenerators with FEC, the FEC itself and the associated digital signal processing (DSP) can consume more than 20% of the total energy [27]. Due to the cost and energy constraints, some 3R regenerators may not have FEC capability. To minimize energy consumption, we assume that FEC functionality is only available at the end nodes of each lightpath. To this end, the BER estimation model that we use in this study considers BER transfer through 1R/2R/3R regenerators [21]. Notice that without the retiming functionality, an all-optical 2R regenerator does not perform as well as an O/E/O 3R regenerator. Hence, we need to consider different BER transfers for the cases when signals are going through different types of regenerators. The details on the BER estimation model that we use in this study can be found in [21] and [24]. The transmission impairments are modeled with link-based metrics, similar to the approaches in [28] and [29]. The dynamic impairments, such as crosstalk and cross-phase modulation, are com-

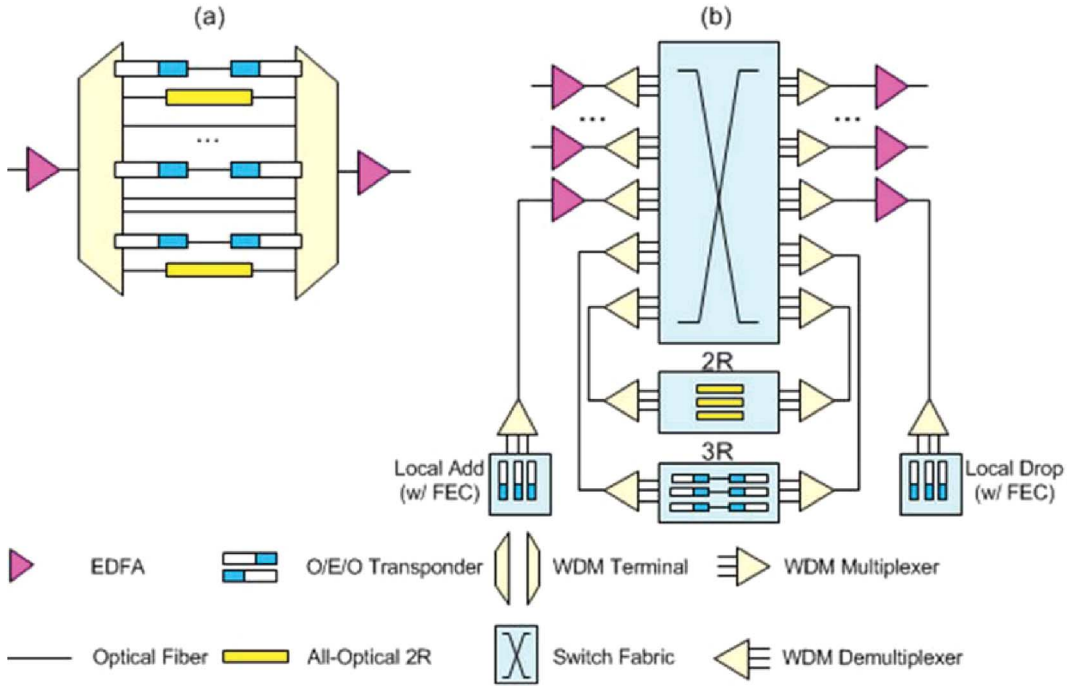

Fig. 1. Architectures of (a) regeneration site and (b) switching node built with MRP.

pensated with a network-wide margin on the end-to-end QoT requirement.

We use $\mathrm{BER}_{s,d,l}$ to denote the end-to-end BER of the lth lightpath from s to d. The QoT requirement is defined as a BER threshold BER_t. In addition to $\mathrm{BER}_{s,d,l}$, another performance parameter of a lightpath is how much power it consumes due to 2R and 3R regenerations in its intermediate nodes. The average energy cost per regenerator is denoted as P_{2R} and P_{3R}, for 2R and 3R regenerators, respectively. Hence, energy-efficient MRP operation of a lightpath has to balance the tradeoff between BER and energy cost, and can be formulated as

$$\min_{f^{i,u}_{s,d,l}} \quad P_R = P_{2\mathrm{R}} \sum_u f^{2,u}_{s,d,l} + P_{3\mathrm{R}} \sum_u f^{3,u}_{s,d,l}, u \in R_{s,d,l} \quad (1)$$

$$\text{s.t.} \quad \mathrm{BER}_{s,d,l} < \mathrm{BER}_t \quad (2)$$

$$\sum_i f^{i,u}_{s,d,l} = 1 \quad \forall u \in R_{s,d,l} \quad (3)$$

where $R_{s,d,l}$ denotes the set of intermediate nodes of the lightpath, and (3) is for the single-connection constraint at each node.

B. MRP With Periodic Placements

To optimize QoT-energy tradeoff for a lightpath, the MRP algorithm has to consider possible placement of 1R, 2R, or 3R regenerator at each intermediate node (i.e., regeneration site or switching node), and thus, the search space grows exponentially with the number of intermediate nodes. If we also consider the complexity of BER estimation, the MRP algorithm using exhaustive search will become impractical when the number of intermediate nodes is large (e.g., >15). To overcome this, we develop a MRP algorithm that combines exhaustive search with periodic regenerator placements based on a 2R/3R ratio $\eta_{2\mathrm{R}/3\mathrm{R}}$. The $\eta_{2\mathrm{R}/3\mathrm{R}}$ of the lth lightpath from s to d is defined as

$$\eta_{2\mathrm{R}/3\mathrm{R}} = \frac{\sum_{i=2}^{3} \sum_u f^{i,u}_{s,d,l}}{|R_{s,d,l}|}, u \in R_{s,d,l}. \quad (4)$$

Typically, based on $R_{s,d,l}$ and the related link-based metrics, we can estimate the upper bound of $\eta_{2\mathrm{R}/3\mathrm{R}}$ such that if we place 1R and 3R regenerators with a periodic arrangement according to it (i.e., place 3R regenerators at fixed intervals along the path), the QoT requirement can be satisfied (i.e., $\mathrm{BER}_{s,d,l} < \mathrm{BER}_t$) [20]. *Algorithm 1* shows the details of the MRP with periodic placements (MRP-Periodic). Specifically, the MRP-Periodic algorithm first determines the placement of 1R and 3R regenerators based on the upper bound of $\eta_{2\mathrm{R}/3\mathrm{R}}$, and then tries to replace as many as 3R regenerators with 1R or 2R regenerators under the QoT constraint for energy saving.

Algorithm 1 MRP Algorithm Based on the Combination of Periodic Placements and Exhaustive Search

collect $R_{s,d,l}$ and link-based metrics;
determine the upper-bound of $\eta_{2\mathrm{R}/3\mathrm{R}}$;
place 3R in the intermediate nodes with a periodic arrangement such that $\eta_{2\mathrm{R}/3\mathrm{R}}$ can satisfy its upper-bound;
place 1R in the rest of the intermediate nodes;
while TRUE **do**
  $m = 1$, $ber[\ldots] \leftarrow \emptyset$, $pos[\ldots] \leftarrow \emptyset$;
  for all u with $f^{3,u}_{s,d,l} = 1$ **do**
    replace the 3R in u with a 1R;
    calculate $\mathrm{BER}_{s,d,l}$ with the replacement;
    $ber[m] = \mathrm{BER}_{s,d,l}$, $pos[m] = u$, $m = m + 1$;
    revert the replacement;
  end for
  if $\min(ber[1 \ldots m-1]) < \mathrm{BER}_t$ **then**
    determine m that $ber[m] = \min(ber[1 \ldots m-1])$;
    replace the 3R in $u = pos[m]$ with a 1R;
  else
    break while-loop;
  end if

19: **end while**
20: **while** TRUE **do**
21: $m = 1$, $ber[\ldots] \leftarrow \emptyset$, $pos[\ldots] \leftarrow \emptyset$;
22: **for** all u with $f_{s,d,l}^{3,u} = 1$ **do**
23: replace the 3R in u with a 2R;
24: calculate $\mathrm{BER}_{s,d,l}$ with the replacement;
25: $ber[m] = \mathrm{BER}_{s,d,l}$, $pos[m] = u$, $m = m + 1$;
26: revert the replacement;
27: **end for**
28: **if** $\min(ber[1 \ldots m-1]) < \mathrm{BER}_t$ **then**
29: determine m that $ber[m] = \min(ber[1 \ldots m-1])$;
30: replace the 3R in $u = pos[m]$ with a 2R;
31: **else**
32: break while-loop;
33: **end if**
34: **end while**

C. MRP With Genetic Algorithm

The MRP optimization can also be implemented with a genetic algorithm (GA) as proposed in [30]. The GA is a search strategy that mimics natural evolution. With proper genetic encoding, a possible MRP solution is represented by a set of genes, called individual chromosome. Fig. 2 shows the genetic encoding scheme. With this scheme, a set of individuals are randomly generated as the initial population. The GA then applies selection, crossover, and mutation iteratively to modify the population consistently, until the algorithm has converged. In each iteration, the GA evaluates each individual (i.e., each MRP solution) with a fitness function defined as

$$F_{s,d,l} = f(\mathrm{BER}_{s,d,l}) + \frac{P_R}{|R_{s,d,l}|} \tag{5}$$

where $f(\mathrm{BER}_{s,d,l})$ has a formulation of

$$f(\mathrm{BER}_{s,d,l}) = \begin{cases} 0, & \mathrm{BER}_{s,d,l} < \mathrm{BER}_t \\ M, & \mathrm{BER}_{s,d,l} \geq \mathrm{BER}_t \end{cases} \tag{6}$$

where $M > P_{3R}$ is a large positive integer for punishing the MRP solutions with $\mathrm{BER}_{s,d,l} \geq \mathrm{BER}_t$. Through the iterations, the GA tries to minimize $F_{s,d,l}$ for the best energy efficiency. Compared to the one in [30], the MRP-GA discussed here has two improvements. First, we modify the fitness function to obtain individuals with higher energy efficiency. Second, we design the mutation operation with an adaptive scheme to improve the GA's search efficiency. Specifically, we change an individual's mutation probability based on its fitness, in a way such that the fitter an individual is (i.e., it represents a MRP solution with higher energy-efficiency), the less possible it is for the GA to modify it.

The simulation results in Fig. 4 indicate that for a lightpath with 30 intermediate nodes, the MRP-GA has converged within 50 iterations. Moreover, MRP-GA can obtain multiple qualified MRP solutions with better energy efficiency, compared to the MRP-Periodic.

D. MRP With Ant Colony Optimization

In addition to MRP-GA, we also develop a MRP algorithm based on ant colony optimization (ACO). Fig. 3 illustrates the working principle of MRP-ACO. For the lth lightpath from s to d, we first construct an auxiliary graph $G'(V', E', T)$ and insert three virtual nodes $u^i, i = 1, 2, 3$, for each intermediate node $u \in R_{s,d,l}$, representing possible placement of 1R, 2R, or 3R regenerator. For any two adjacent nodes u and v in $R_{s,d,l}$, their virtual nodes u^i and v^i in G' are fully connected. Here, T represents the set of pheromones $\{\tau_{e'}\}$ on each link $e' \in E'$. The pheromone $\tau_{\{u',v'\}}$ reflects the probability that an ant will choose $\{u', v'\}$ in its path finding in the auxiliary graph for MRP-ACO. For all $\{u', v'\}$ origins from a node u' in G', we have

$$\sum_{v'} \tau_{\{u',v'\}} = 1, [v' : \{u', v'\} \in E']. \tag{7}$$

Initially, the pheromone $\{\tau_{e'}\}$ on each link $e' \in E'$ is identical. The MRP-ACO sends certain amount of ants from s and lets them move toward d in a random but nonreturn way according to T. When an ant reaches d, a MRP solution is formed and its fitness is calculated with (5) and (6). *Algorithm 2* shows the details of the MRP-ACO. Fig. 4 shows the evolution of the best fitness in the optimizations with MRP-GA and MRP-ACO. In the simulations, we assume that the data rate is 40 Gb/s, the fiber transmission distance between two intermediate nodes is identical as 300 km, $\mathrm{BER}_t = 10^{-4}$ is the QoT requirement before FEC at d, and the average energy cost per 2R and 3R regenerator are $P_{2R} = 2$ units and $P_{3R} = 15$ units. The energy-cost ratio between all-optical 2R and O/E/O 3R regenerators is determined based on the results in [17] and [31]. It can be seen that for this lightpath arrangement, MRP-GA converges faster than MRP-ACO, but MRP-ACO obtains MRP solutions with slightly smaller fitness (i.e., better energy efficiency).

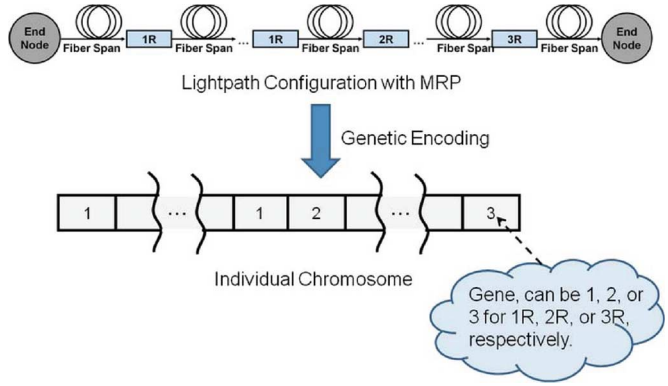

Fig. 2. Genetic encoding for MRP optimization with GA.

Algorithm 2 MRP Algorithm Based on ACO

collect $R_{s,d,l}$ and link-based metrics;
construct the auxiliary graph G';
deposit initial pheromone T on $e' \in E'$;
$m = 1$;
while $m < m_{MAX}$ **do**
  for all ants **do**
    $u' = s$;
    while $u' \neq d$ **do**
      ant pick the next hop v' randomly based on $\tau_{\{u',v'\}}$;
      $u' = v'$;
    end while

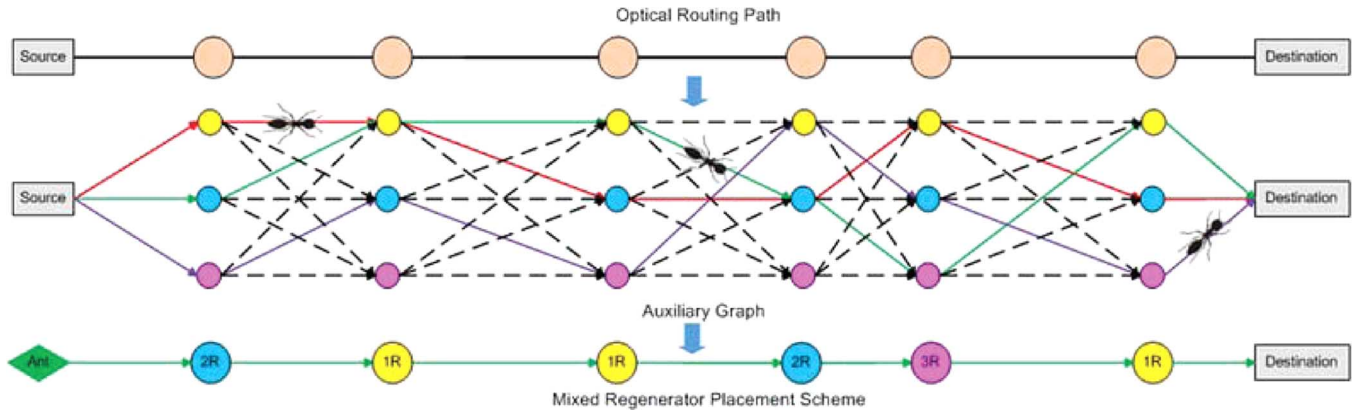

Fig. 3. ACO of MRP along a lightpath using an auxiliary graph.

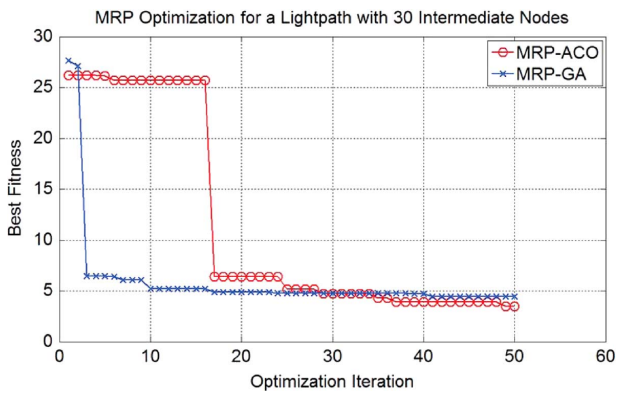

Fig. 4. Evolutions of the best fitness in MRP optimizations with MRP-GA and MRP-ACO.

12: calculate $\mathrm{BER}_{s,d,l}$ and P_R of the MRP obtained by the ant;
13: calculate fitness of the MRP with (5)–(6);
14: **end for**
15: sort fitness of the MRP from the ants;
16: update pheromone T to give preference to the MRP with the smallest fitness;
17: normalize T to satisfy (7);
18: $m = m + 1$;
19: **end while**

III. Energy-Efficient Network Planning With Joint Optimization of MRP and RWA

A. Problem Formulation

Based on the path-based impairment-aware MRP algorithms discussed in Section II, energy-efficient translucent network planning can be achieved with joint optimization of MRP and RWA. We define the problem of energy-efficient translucent network planning as follows: given $G(V, E)$ and a traffic matrix $\Lambda_{s,d}$, perform RWA and MRP such that all traffic requests can be served with desired QoT requirement and the total energy cost of 2R and 3R regenerators in the network is minimized. The problem can be considered as an offline one, as the traffic matrix is known *a priori*. We use the following notations to describe the problem:

$G(V, E)$	WDM network topology.
V	Set of nodes.
E	Set of fiber links.
W	Set of wavelength channels.
$\Lambda_{s,d}$	Traffic matrix.
$\lambda_{s,d}$	Traffic request from s to d, $\lambda_{s,d} \in \Lambda_{s,d}$.
$LR_{s,d,l}$	lth lightpath from s to d, $s, d \in V$.
$\mathrm{BER}_{s,d,l}$	End-to-end BER of $\mathrm{LR}_{s,d,l}$.
$R_{s,d,l}$	Set of intermediate nodes in the routing path of $\mathrm{LR}_{s,d,l}$.
$f_{s,d,l}^{i,u,w}$	Flag of MRP, $f_{s,d,l}^{i,u,w} = 1$ if the signal of $\mathrm{LR}_{s,d,l}$ on input wavelength $w \in W$ is regenerated by i-R type regenerator at intermediate node $u \in V$; otherwise, $f_{s,d,l}^{i,u,w} = 0$.
$q_{s,d,l}^{u,v,w}$	Flag of RWA, $q_{s,d,l}^{u,v,w} = 1$ if the signal of $\mathrm{LR}_{s,d,l}$ is routed over link $\{u, v\} \in E$ with wavelength $w \in W$; otherwise, $q_{s,d,l}^{u,v,w} = 0$.
BER_t	End-to-end BER threshold from the QoT requirement.
$P_{2\mathrm{R}}$	Average energy cost per 2R.
$P_{3\mathrm{R}}$	Average energy cost per 3R.

With these notations, we formulate the energy-efficient translucent network planning using joint optimization of MRP and RWA as follows.

Objective:

$$\min \sum_{s,d} \sum_{l} \sum_{w} \sum_{u \in R_{s,d,l}} \left(P_{2\mathrm{R}} \cdot f_{s,d,l}^{2,u,w} + P_{3\mathrm{R}} \cdot f_{s,d,l}^{3,u,w} \right). \tag{8}$$

Subject to the Following Constraints:

1) The end-to-end BER of all lightpaths should satisfy the QoT requirement

$$\mathrm{BER}_{s,d,l} < \mathrm{BER}_t \quad \forall s, d, l. \tag{9}$$

2) The wavelength assignment at each fiber link should not exceed its capacity

$$\sum_{s,d} \sum_{l} \sum_{w} q_{s,d,l}^{u,v,w} \le |W| \quad \forall \{u, v\} \in E. \tag{10}$$

3) A wavelength should only be used once on a fiber link to avoid wavelength contention

$$\sum_{s,d} \sum_{l} q_{s,d,l}^{u,v,w} \le 1 \quad \forall \{u, v\} \in E, w \in W. \tag{11}$$

4) A regenerator should only be used by one lightpath to avoid component contention

$$\sum_{s,d}\sum_{l} f_{s,d,l}^{i,u,w} \le 1 \quad \forall i, u \in V, w \in W. \tag{12}$$

5) A lightpath should be routed over a single routing path

$$\sum_{w}\left(\sum_{u} q_{s,d,l}^{u,v,w} - \sum_{j} q_{s,d,l}^{v,j,w}\right) = \begin{cases} -1, & v = s \\ 1, & v = d \ \forall s,d,l \\ 0, & \text{otherwise.} \end{cases} \tag{13}$$

6) In this offline network planning, we consider the light traffic case where the network resource is enough to support the traffic matrix $\Lambda_{s,d}$, and no request blocking will occur. Hence, all traffic requests should be served

$$\sum_{w,l}\left(\sum_{u} q_{s,d,l}^{u,v,w} - \sum_{j} q_{s,d,l}^{v,j,w}\right) = \begin{cases} -\lambda_{s,d}, & v = s \\ \lambda_{s,d}, & v = d \ \forall s,d. \end{cases} \tag{14}$$

7) We need to consider the wavelength continuity constraint when a lightpath experiences a 1R regenerator at an intermediate node. Specifically, for an intermediate node u, if the lightpath $\mathrm{LR}_{s,d,l}$ comes in on link $\{v_i, u\}$ and goes out on link $\{u, v_o\}$, we need to satisfy the following equation:

$$q_{s,d,l}^{v_i,u,w} = q_{s,d,l}^{u,v_o,w} = 1, \quad \left\{u, w : f_{s,d,l}^{1,u,w} = 1\right\}. \tag{15}$$

Notice that our formulation is not an ILP, as the calculation of $\mathrm{BER}_{s,d,l}$ is nonlinear. However, after the MRP along a routing path has been determined with the algorithms discussed in Section II, it is transferred to an ILP formulation. Due to the complexity of the problem, we resort to a heuristic algorithm to solve it.

B. Heuristic Algorithm

The proposed heuristic algorithm relies on several phases to solve the offline network planning with joint optimization of MRP and RWA. *Algorithm 3* illustrates the details of the offline network planning. In Phase 1, we use a *K*-shortest path algorithm to determine K routing path candidates for each s–d pair in $G(V, E)$. The MRP along each candidate is then determined with one of the MRP algorithms discussed in Section II, as explained in lines 4–7 of *Algorithm 3*.

Phase 2 is for joint optimization of MRP and RWA to serve the traffic requests. In lines 13–20, we implement the precomputed MRP in a routing path candidate and resolve potential component contentions by moving the 2R/3R regenerator to intermediate nodes near the contention nodes. In lines 21–35, we perform wavelength assignment for each candidate with a maximum transparent segment length (MTSL) approach to minimize wavelength contentions. We assume that both 2R and 3R regenerators are capable of wavelength conversion, and thus, the wavelength continuity constraint only applies to the segment between two 2R/3R regenerators in a routing path.

Fig. 5 illustrates an intuitive example of the MTSL approach. Within a routing path, there is a segment that covers eight links, and the fiber links support eight wavelengths. The slots filled with colors are those occupied by other lightpaths. With the link status

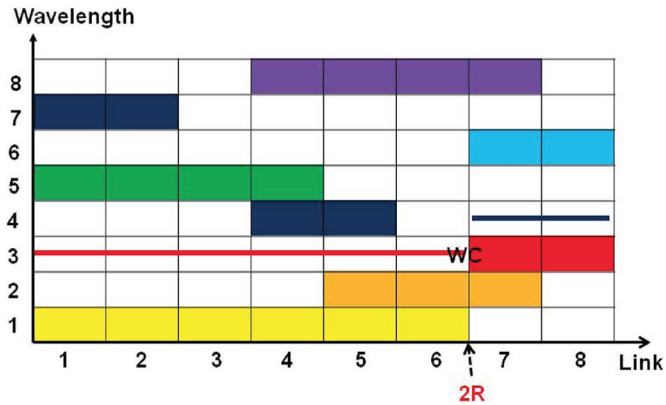

Fig. 5. Example of wavelength assignment with the MTSL approach.

in Fig. 5, we can see that the longest segment length we can obtain is 6 links, by using wavelength 3. Therefore, the MTSL approach assigns the lightpath to wavelength 3 for links 1–6, places a 2R regenerator between links 6 and 7 to resolve wavelength contention, and picks wavelength 4 for links 7 and 8.

When the MRP and RWA are done for each routing path candidate, the end-to-end BER is calculated to validate them. Among all valid candidates, the one with the minimal energy cost is chosen to serve the lightpath. The whole process is then repeated until all traffic requests are served.

Algorithm 3 Energy-Efficient Translucent Network Design With Joint Optimization of MRP and RWA

Phase 1: Collect physical status and perform pre-computation
1: collect link-based metrics of $G(V, E)$;
2: **for** all s-d pairs in $G(V, E)$, $s, d \in V$ **do**
3: calculate K shortest routing paths;
4: **for** all routing paths **do**
5: perform MRP with MRP-Periodic, MRP-GA, or MRP-ACO;
6: record MRP result;
7: **end for**
8: **end for**

Phase 2: Perform MRP and RWA to serve traffic requests
9: **while** there are unserved traffic requests in $\Lambda_{s,d}$ **do**
10: get the s-d pair of the lightpath $\mathrm{LR}_{s,d,l}$;
11: load the pre-computed K routing path candidates from s to d;
12: **for** all routing path candidates **do**
13: load the pre-computed MRP;
for all intermediate nodes $u \in R_{s,d,l}$ **do**
15: implement the pre-computed MRP;
16: **if** there is a component contention **then**
17: find the nearest node v in $R_{s,d,l}$ where the pre-computed MRP places a 1R;
18: replace the 1R in v with the 2R/3R that supposes to be in u;
19: **end if**
20: **end for**
21: $u = s$, $w_{in} = \emptyset$;
22: **while** $u \neq d$ **do**

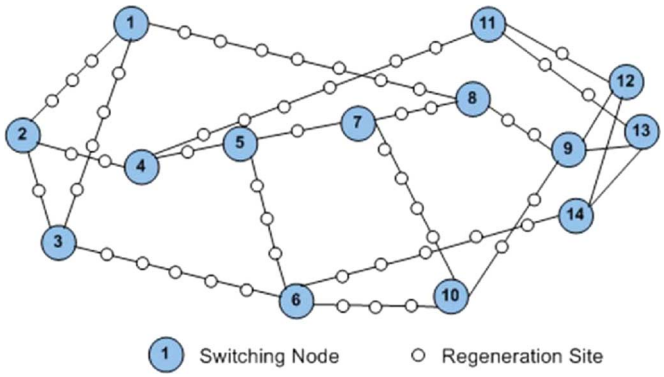

Fig. 6. NSFNET topology for simulations.

23: get $e = \{u, v\}$ from the routing path candidate;
24: **if** $u \neq s$ AND MRP has $f_{s,d,l}^{1,u,w_{in}} = 1$ **then**
25: **if** w_{in} is not available on e **then**
26: $f_{s,d,l}^{2,u,w_{in}} = 1$;
27: **end if**
28: **end if**
29: **for** all available wavelength $w \in W$ on e **do**
30: get the transparent segment of w;
31: **end for**
32: assign $LR_{s,d,l}$ to the w that achieve the longest transparent segment;
33: $w_{in} = w$;
34: set u to the end-node of the transparent segment;
35: **end while**
36: calculate $\text{BER}_{s,d,l}$ of the routing path candidate;
37: **if** $\text{BER}_{s,d,l} < \text{BER}_t$ **then**
38: record the routing path candidate as valid;
39: calculate the energy-cost of the routing path candidate with (1);
40: **end if**
41: **end for**
42: sort valid routing path candidates according to their energy-costs;
43: serve $LR_{s,d,l}$ using the routing path candidate that has the minimal energy-cost;
44: **end while**

C. Performance Evaluation

We perform simulations to evaluate the performance of the energy-efficient network planning heuristic. The simulation parameters are listed in Table II, and Fig. 6 shows the NSFNET topology used in the simulations. There are two types of nodes in the topology: 1) switching nodes (labeled with numbers) with the architecture shown in Fig. 1(b) and 2) by-pass regeneration sites with the architecture shown in Fig. 1(a).

The simulations generate lightpath requests by choosing the s–d pairs randomly. With the same amount of requests, we first compare our translucent network planning with MRP to the traditional one without all-optical 2R regenerators, and Fig. 7 shows the simulation results. The MRP are obtained with the MRP-Periodic algorithm. To obtain each data point in Fig. 7, we average the results from ten different lightpath request sets. It can be seen that the MRP scheme achieves significant energy saving (62.26% in average), compared to the traditional one without all-optical 2R regenerators. For the traditional scheme, the average number of 3R regenerators required per request is 2.29, while it is 0.54 for the MRP-Periodic scheme. To achieve this amount of reduction on O/E/O 3R regenerators, the MRP-Periodic scheme needs 2.99 all-optical 2R regenerators per request.

TABLE I
SIMULATION PARAMETERS

Output power per wavelength channel	0 dBm
Fiber loss	0.25 dB/km
PMD parameter	0.1 $ps/\sqrt{km}$
EDFA noise figure	6 dB
EDFA spacing	75 km
Fiber link length between nodes	150, or 300 km
$\|W\|$, wavelengths per fiber link	40
K, number of routing path candidates	5
Data rate	40 Gb/s
BER_t	10^{-4}
P_{2R}	2 units
P_{3R}	15 units

TABLE II
COMPARISONS OF TRANSLUCENT NETWORK DESIGNS

	Traditional Scheme	MRP-Periodic	MRP-ACO	MRP-GA
2R per request	0	2.99	3.40	3.95
3R per request	2.29	0.54	0.29	0.08
Average energy-saving	0	58.91%	67.67%	73.62%

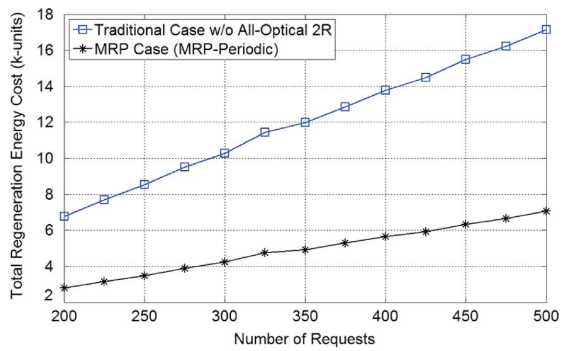

Fig. 7. Total regeneration energy costs of the translucent networks designed with the traditional scheme without all-optical 2R regenerators and the MRP-Periodic scheme.

We then compare the network designs with different MRP algorithms, and Fig. 8 shows the simulation results. We observe that the networks designed with the regenerator placements from MRP-GA have the smallest regeneration energy costs. Table II summarizes the average numbers of 2R and 3R regenerators per requests for different network design schemes. Under the same QoT constraint, the MRP-GA scheme tends to replace the most O/E/O 3R regenerators with all-optical 2R regenerators, and therefore achieves the best energy efficiency.

IV. PROVISIONING OF TRANSLUCENT NETWORKS WITH MRP

For online provisioning of the translucent networks with MRP, we assume that the 2R and 3R regenerators have already been placed in the network using the joint optimization of MRP and RWA discussed in Section III. To consider the CAPEX restrictions, we fix the total regeneration energy cost at certain value when using different MRP algorithms to design the translucent networks. The dynamic lightpath requests come

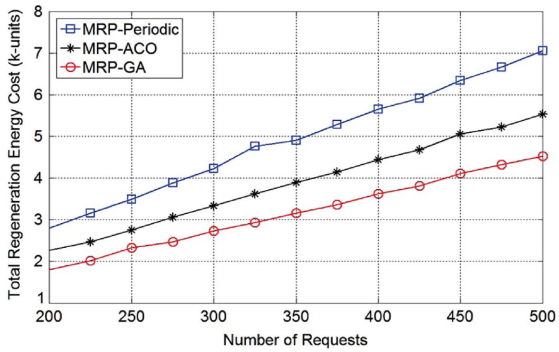

Fig. 8. Total regeneration energy costs of the translucent networks designed with the MRP schemes using different regenerator placement algorithms.

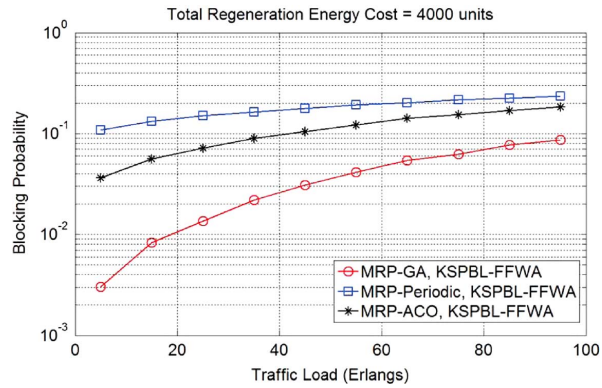

Fig. 9. Blocking probability curves for networks designed with total regeneration energy cost as 4000 units.

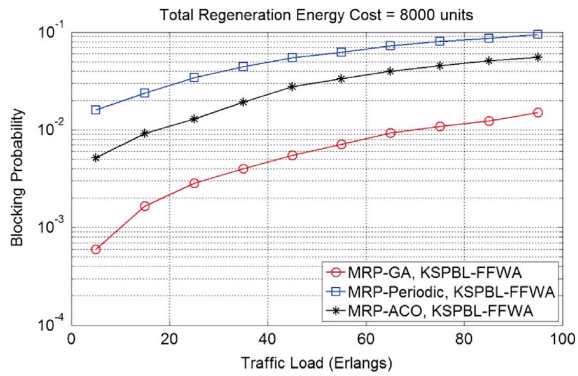

Fig. 10. Blocking probability curves for networks designed with total regeneration energy cost as 8000 units.

in according to a Poisson process with a rate of λ requests per time unit, and the holding time of a request follows an exponential distribution with an average value of μ time units. We then quantify the traffic load with $\lambda \cdot \mu$ in erlangs. Our provisioning algorithms serve the lightpath requests one by one with online RWA and regenerator allocations. To serve a request from s to d, the provisioning algorithm finds a sequence of transparent segments between s and d, allocates regenerators at intermediate nodes, and make sure that the QoT is acceptable, i.e., end-to-end BER is less than BER_t. The objective of online provisioning is to minimize the blocking probability, while satisfying the resource (e.g., wavelength channels and regenerators) and QoT constraints.

Algorithm 4 shows the procedures of the proposed online provisioning algorithms for translucent networks with MRP. In line 1, the precomputation phase is the same as that in *Algorithm 3*. We precompute K shortest paths for each s–d pair and perform MRP using MRP-Periodic, MRP-ACO, or MRP-GA. Specifically, we use the same MRP algorithm that a network was designed for online provisioning. In lines 5–33, the routing path selection incorporates a K-shortest paths and balanced-load scenario to distribute the traffic load evenly in a network and to minimize the blocking probability. In line 34, the wavelength assignment is performed based on each transparent segment, i.e., a sequence of links between the source and a 2R/3R regenerator, two 2R/3R regenerators, or a 2R/3R regenerator and the destination. We implement the first-fit wavelength assignment (FFWA) in the online provisioning. With the FFWA, the provisioning algorithm chooses the available wavelength channel that has the lowest index to serve the lightpath request.

To evaluate the proposed provisioning algorithms, we perform simulations of dynamic requests in the NSFNET topology shown in Fig. 6. The simulation parameters are the same as those in Table I. The purpose of the evaluation is to compare the request blocking probability of networks designed with different MRP algorithms, when the energy budget on signal regeneration is the same. Since a request can be blocked due to either wavelength limitations (i.e., the wavelength continuity cannot be satisfied or the wavelength channels are used up on a link) or component shortages (i.e., the 2R/3R regenerators at an intermediate nodes are used up), we consider both situations in the simulations. We first fix the total regeneration energy cost at 4000 or 8000 units, and design the networks with different MRP algorithms. Then, we try to provision 10 000 dynamic requests for each traffic load case to obtain the curve of the blocking probability. Figs. 9 and 10 show the simulation results for networks designed with total regeneration cost at 4000 and 8000 units, respectively. It can be seen that in both cases, the networks designed with MRP-GA achieve the smallest blocking probability in the online provisioning.

In simulations, we notice that the component contentions due to limited 2R/3R regenerators at intermediate nodes can result in request blocking. Notice that to satisfy the end-to-end QoT, the MRP for a lightpath is not unique. In [30], we showed that MRP-GA can obtain multiple qualified MRP solutions for a lightpath simultaneously. Hence, we precompute N qualified MRP solutions for each lightpath and design an online provisioning algorithm with multiple MRP to avoid component contentions. *Algorithm 5* shows the details of regenerator allocation using multiple MRP solutions. *Algorithm 5* can be used to replace lines 7–13 in *Algorithm 4* to achieve online provisioning using multiple MRP. We compare its performance with provisioning using a single MRP in networks designed with MRP-GA, and Fig. 11 shows the results. In the simulations, we choose $N = 5$. We can see that the multiple MRP scheme further reduces the blocking probability.

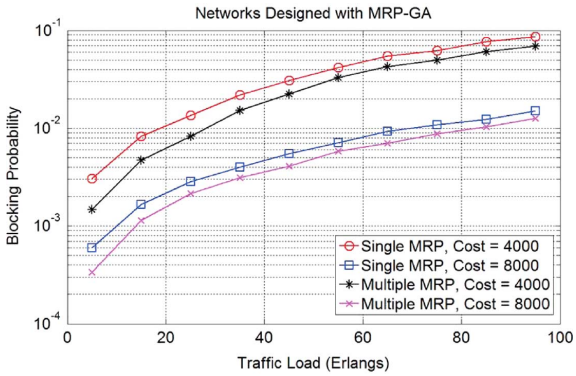

Fig. 11. Blocking probability curves for networks designed with MRP-GA provisioned with single/multiple MRP schemes.

Algorithm 4 Online Provisioning of a Translucent Network With MRP

run **Phase 1** of *Algorithm 3*;
while the network is operational **do**
  restore network resources used by expired requests;
  get the s-d pair and holding-time Δt of a new request $LR_{s,d,\Delta t}$;
  load the pre-computed K routing path candidates from s to d;
  for all path candidates **do**
    load the pre-computed MRP;
    for all intermediate nodes **do**
      allocate 2R/3R using the pre-computed MRP;
      if there is a component contention **then**
        mark the path candidate as invalid;
      end if
    end for
    if the path candidate is valid **then**
      for each transparent segment l along the path **do**
        find the number of unused wavelengths w_l on l;
        set the weight of segment l as w_l;
      end for
      set the weight of the path candidate as $\min(\{w_l\}), \forall l$;
      if the weight of the path candidate is 0 **then**
        mark the path candidate as invalid;
      end if
    end if
  end for
  if there are one or more valid path candidates **then**
    sort path candidates according to their weights;
    find the path candidate(s) with the maximum weight;
    if obtain multiple path candidates **then**
      choose the path candidate with the minimum energy-cost;
      else
        choose the path candidate;
      end if
      perform first-fit wavelength assignment for each transparent segment in the selected path candidate;
      update network status accordingly;
    else
      mark the request as blocked;
    end if
end while

Algorithm 5 Regenerator Allocation Using Multiple MRP

for all qualified MRP with energy-costs from low to high **do**
  $flag = \text{TRUE}$;
  for all intermediate nodes **do**
    allocate 2R/3R using the pre-computed MRP;
    if there is a component contention **then**
      $flag = \text{FALSE}$;
      break for-loop;
    end if
  end for
  if $flag = \text{TRUE}$ **then**
    break for-loop;
  end if
end for
if $flag = \text{FALSE}$ **then**
  mark the path candidate as invalid;
end if

V. Conclusion

In this paper, we showed that the energy cost of a translucent network could be further reduced by leveraging the energy efficiency of all-optical 2R regenerators. The investigation was focused on a translucent network infrastructure that used all-optical 2R regenerators to partially replace O/E/O 3R regenerators and incorporated MRP. We designed three path-based impairment-aware MRP algorithms based on periodic placement, GA and ACO, and compared their performance in offline network planning. The offline network planning was based on a heuristic algorithm that could achieve joint optimization of MRP and RWA for high energy efficiency. Simulation results showed that the algorithm achieved 58.91–73.62% saving on the regeneration energy. The results also indicated that networks designed with the MRP-GA had the best energy efficiency. We then investigated the online provisioning problem of the translucent networks with MRP, and proposed several algorithms to serve dynamic requests with low blocking probability. Simulation results indicated that the online provisioning algorithm that combined MRP-GA and the multiple MRP scheme achieved the lowest blocking probability.

References

[1] B. Ramamurthy *et al.*, "Transparent vs. opaque vs. translucent wavelength-routed optical networks," in *Proc. Optical Fiber Commun. Conf.*, Feb. 1999, pp. 59–61, paper TuF2.

[2] B. Ramamurthy *et al.*, "Translucent optical WDM networks for the next-generation backbone networks," in *Proc. IEEE Global Telecommun. Conf.*, Nov. 2001, pp. 1–5.
[3] C. Saradhi *et al.*, "Practical and deployment issues to be considered in regenerator placement and operation of translucent optical networks," in *Proc. Int. Conf. Transparent Optical Netw.*, 2010, paper Th.A.1.2.
[4] X. Yang *et al.*, "Dynamic routing in translucent WDM optical networks: The intradomain case," *J. Lightw. Technol*, vol. 23, no. 3, pp. 955–971, Mar. 2005.
[5] N. Shinomiya *et al.*, "Hybrid link/path-based design for translucent photonic network dimensioning," *J. Lightw. Technol.*, vol. 25, no. 10, pp. 2931–2941, Oct. 2007.
[6] S. Pachnicke *et al.*, "Physical impairment based regenerator placement and routing in translucent optical networks," in *Proc. Optical Fiber Commun. Conf.*, Mar. 2008, paper OWA2.
[7] K. Manousakis *et al.*, "Offline impairment-aware routing and wavelength assignment algorithms in translucent WDM optical networks," *J. Lightw. Technol.*, vol. 27, no. 12, pp. 1866–1877, Jun. 2009.
[8] K. Manousakis *et al.*, "Joint online routing, wavelength assignment and regenerator allocation in translucent optical networks," *J. Lightw. Technol.*, vol. 28, no. 8, pp. 1152–1163, Apr. 2010.
[9] G. Shen *et al.*, "Sparse traffic grooming in translucent optical networks," *J. Lightw. Technol.*, vol. 27, no. 20, pp. 4471–4479, Oct. 2009.
[10] A. Nag *et al.*, "Transparent vs. translucent optical network design with mixed line rates," in *Proc. Optical Fiber Commn. Conf.*, Mar. 2009, paper OWI7.
[11] R. Martinez *et al.*, "Experimental translucent-oriented routing for dynamic lightpath provisioning in GMPLS-enabled wavelength switched optical networks," *J. Lightw. Technol.*, vol. 28, no. 8, pp. 1241–1255, Apr. 2010.
[12] S. Azodolmolky *et al.*, "A novel impairment aware RWA algorithm with consideration of QoT estimation inaccuracy," *J. Opt. Commun. Netw.*, vol. 3, pp. 290–299, Apr. 2011.
[13] S. Azodolmolky *et al.*, "Experimental demonstration of an impairment aware network planning and operation tool for transparent/translucent optical networks," *J. Lightw. Technol.*, vol. 29, no. 4, pp. 439–448, Feb. 2011.
[14] D. Shen *et al.*, "Efficient regenerator placement and wavelength assignment in optical networks," in *Proc. Optical Fiber Commun. Conf.*, Mar. 2011, paper OThAA4.
[15] Y. Zhu *et al.*, "Efficient impairment-constrained 3R regenerator placement for light-trees in optical networks," *J. Opt. Commun. Netw.*, vol. 3, pp. 359–371, Apr. 2011.
[16] N. Sambo *et al.*, "Encompassing ROADM add/drop constraints in GMPLS-based WSONs," *Eur. Trans. Telecommun.*, vol. 23, pp. 86–95, Jan. 2012.
[17] O. Leclerc *et al.*, "Optical regeneration at 40 Gb/s and beyond," *J. Lightw. Technol.*, vol. 21, no. 11, pp. 2779–2790, Nov. 2003.
[18] Z. Zhu *et al.*, "43 Gb/s 264 km field fiber transmission using 2R regeneration in a tunable all-optical signal regenerator," in *Proc. Conf. Laser Electro-Optics*, May 2005, paper CTuO3.
[19] G. Maxwell, "Hybrid integration technology for high functionality devices in optical communications," in *Proc. Optical Fiber Commun. Conf.*, Mar. 2008, paper OWI3.
[20] Z. Zhu, "Design green and cost-effective translucent optical networks," in *Proc. Optical Fiber Commun. Conf.*, Mar. 2011, paper OWI4.
[21] Z. Zhu, "Mixed placement of 1R/2R/3R regenerators in translucent optical networks to achieve green and cost-effective design," *IEEE Commun. Lett*, vol. 15, no. 7, pp. 752–754, Jul. 2011.
[22] Z. Zhu *et al.*, "Joint optimization of mixed regenerator placement and wavelength assignment for green translucent optical networks," in *Proc. Asia Commun. Photon. Conf. and Exhib.*, Nov. 2011, paper 8310–8315.
[23] W. Zhong *et al.*, "Design energy efficient translucent optical networks with joint routing and wavelength assignment and mixed regenerator placement," in *Proc. Optical Fiber Commun. Conf.*, Mar. 2012, paper JTh2A.46.
[24] Z. Zhu *et al.*, "Jitter and amplitude noise accumulations in cascaded all-optical regenerators," *J. Lightw. Technol.*, vol. 26, no. 12, pp. 1640–1652, Jun. 2008.
[25] P. Ohlen *et al.*, "Noise accumulation and BER estimates in concatenated nonlinear optoelectronic repeaters," *IEEE Photon. Technol. Lett*, vol. 9, no. 7, pp. 1011–1013, Jul. 1997.
[26] Z. Zhu *et al.*, "High-performance all-optical 3R regeneration for scalable fiber transmission system applications," *J. Lightw. Technol.*, vol. 25, no. 2, pp. 504–511, Feb. 2007.
[27] M. Annalisa *et al.*, "Power management of optoelectronic interface for dynamic optical networks," in *Proc. Eur. Conf. and Exhib. Optical Commun.*, Sept. 2011, paper We.8.K.3.
[28] T. Tsuritani *et al.*, "Optical path computation element interworking with network management system for transparent mesh networks," in *Proc. Optical Fiber Commun.*, Mar. 2008, paper NWF5.
[29] S. Rai *et al.*, "On provisioning in all-optical networks: An impairment-aware approach," *IEEE/ACM Trans. Netw.*, vol. 17, no. 6, pp. 1989–2001, Dec. 2009.
[30] Z. Zhu *et al.*, "Using genetic algorithm to optimize mixed regenerator placement of 1R/2R/3R regenerators in translucent lightpaths for energy-efficient design," *IEEE Commun. Lett*, vol. 16, no. 2, pp. 262–264, Feb. 2012.
[31] M. Murakami *et al.*, "Power consumption analysis of optical cross-connect equipment for future large capacity optical networks," in *Proc. Int. Conf. Transparent Optical Netw.*, 2009, paper We.B2.4.

Zuqing Zhu (M'07–SM'12) received the Ph.D. degree from the Department of Electrical and Computer Engineering, University of California, Davis, in 2007.

From July 2007 to January 2011, he was with the Service Provider Technology Group of Cisco Systems, San Jose, as a Senior R&D Engineer. In January 2011, he joined the University of Science and Technology of China, Anhui, China, where he is currently an Associate Professor. He has published more than 60 papers in peer-reviewed journals and conferences of the IEEE, the Institution of Electrical Engineers, and the Optical Society of America (OSA). His research interests include energy-efficient network designs, access network technologies, and optical communications and networks.

Dr. Zhu has been in the technical program committees of INFOCOM, ICC, GLOBECOM, ICCCN, etc. He is also an editorial board member of *Journal of Optical Switching and Networking* (Elsevier), *Telecommunication Systems Journal* (Springer), *European Transactions on Telecommunications* (Wiley), etc. He is a member of the OSA.

Xiaoliang Chen, biography not available at the time of publication.

Fan Ji, biography not available at the time of publication.

Liang Zhang, biography not available at the time of publication.

Farid Farahmand (M'08) received the Ph.D. degree from the Department of Computer Science, University of Texas at Dallas, Richardson, in 2005.

He is currently an Assistant Professor in the Department of Engineering Science, Sonoma State University, Rohnert Park, CA. He is also the Director of Advanced Internet Technology in the Interests of Society Laboratory. Prior to this position, he was a Research Scientist at Alcatel-Lucent Corporate Research and was involved in the development of terabit optical routers. He holds multiple international patents, numerous reference conference articles and journal publications, and several book chapters, on the subjects of wireless communications, optical networking, green networking, and delay tolerant networks. He is actively involved in many conferences and serves as the Reviewer and Coeditor to a number of technical conferences and journals.

He is a member of the American Society for Engineering Education and the Engineers Without Borders USA.

Jason P. Jue (M'99–SM'04) received the B.S. degree in electrical engineering from the University of California, Berkeley, the M.S. degree in electrical engineering from the University of California, Los Angeles, and the Ph.D. degree in computer engineering from the University of California, Davis, in 1990, 1991, and 1999, respectively.

He is currently a Professor in the Department of Computer Science, University of Texas at Dallas, Richardson. His research interests include optical networks, network control and management, and network survivability.